CHAPTER

12 X-ray diffraction: intensities

> *"The flickering greenish light, crackling and smell of ozone were sufficiently terrifying to impress the incident deeply in a child's mind. When I think, however, of the early experiments, the interest which they aroused in medical men is not their chief significance to me! I see them as fore-runners of my father's interest in the ionization of gases leading to his experiments with X-rays from radium and finally the experiments on the diffraction of X-rays by matter which we carried out together."*
>
> W. L. Bragg, foreword to "Salute to the X-ray Pioneers of Australia"

12.1 Scattering by electrons, atoms, and unit cells

We have seen in the previous chapter how X-rays are generated when an electron is accelerated or decelerated. If a beam of X-rays is incident upon a collection of electrons, either bonded to atoms or in a conduction band, then the electric field associated with the X-rays will force those electrons into oscillation. Because of the forced oscillation, they will emit their own X-rays, and this phenomenon is known as *X-ray scattering*. In the following subsections, we will describe quantitatively how first a single electron, then an atom, and finally a complete unit cell scatters an incident beam of X-rays.

12.1.1 Scattering by a single electron

Consider a single electron located in the origin of a reference frame (Fig. 12.1). Assume that an X-ray beam goes from the negative x-direction towards the electron. An observer is located at the point P, in the $x-z$ plane, at a distance r from the origin, and at an angle 2θ above the $x-y$ plane (one can always

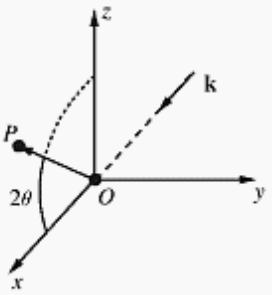

Fig. 12.1. Reference frame used for the computation of single electron scattering.

rotate the reference frame so that this setup is realized). If the incident beam has intensity I_0, then the scattered radiation at the point P can be computed from the *Thomson* equation:

$$\boxed{I = I_0 \frac{\mathrm{K}}{r^2} \sin^2 \alpha,} \tag{12.1}$$

where α is the angle between the scattering direction and the direction of acceleration of the electron. The constant K is given by:

$$\mathrm{K} = \left(\frac{\mu_0}{4\pi}\right)^2 \times \left(\frac{e^4}{m^2}\right) = 7.94 \times 10^{-30} \mathrm{m}^2.$$

This is a very small number, which indicates that the scattering due to a single electron is rather weak. It is only when one brings together large numbers of electrons (of the order of 10^{23} or more) that the scattering becomes easily measurable.

The electric field of an incident X-ray beam will cause the electron to oscillate along a direction parallel to the electric field vector **E**. Since this vector is perpendicular to the propagation direction (which we have taken along the positive x-axis), the vector must be located in the $y-z$ plane. The direction of **E** is known as the *polarization direction*. For a normal X-ray beam, the polarization is random. This means that, on average, the y component of **E** must be equal to the z component. The intensity of an X-ray beam depends quadratically on the magnitude of the electric field, and hence the components of the intensity along the y and z directions must be, on average, equal to each other and equal to half the total intensity. Mathematically this is stated as follows:

$$I_{0y} = I_{0z} = \frac{1}{2} I_0.$$

The average incident X-ray photon can thus be decomposed in a component along y, and a component along z. Let us determine how each of these components contributes to the scattering at the point P. First, we consider the y component. The angle between the y direction and the scattering direction is $\alpha = \pi/2$, from which we find:

$$I_y(P) = I_{0y} \frac{\mathrm{K}}{r^2}.$$

For the z component, the angle α becomes equal to $\pi/2 - 2\theta$ and we find

$$I_z(P) = I_{0z} \frac{\mathrm{K}}{r^2} \cos^2 2\theta.$$

The total scattered intensity at the point P is equal to the sum of the two components:

$$\boxed{I_P = I_0 \frac{\mathrm{K}}{r^2}\left(\frac{1+\cos^2 2\theta}{2}\right).} \tag{12.2}$$

Note that the scattered intensity is strongest for $\theta = 0$ and $\theta = \pi$; it is weakest for $\theta = \pi/2$. The angular factor in Equation 12.2 is known as the *polarization factor*. We will return to this factor later on in this chapter.

From here on, we will assume that the observer is located far from the sample (far compared to the atomic scale) and the factor K/r^2 will not always be explicitly written. Most diffraction experiments do not work with absolute diffracted intensities, but with relative values; one takes the strongest diffraction peak to be the value 100, and re-scales all peaks with respect to this peak. In the re-scaling process, pre-factors such as K/r^2 cancel out against each other.

There is another way in which X-rays can be scattered by an electron. From quantum mechanics we know that a particle can have both particle-like and wave-like properties. The reverse is also true: a wave can in certain situations behave as if it were a particle. This is the reason why we regard electromagnetic rays as particles, or *photons*. As a particle, a photon has a definite momentum and it can transfer part of this momentum in a billiard-like collision with the electron. In doing so, the photon loses part of its energy and therefore it changes its wavelength. Radiation scattered in this manner is known as *Compton modified radiation* and the "collision process" is known as *Compton scattering*. Since the X-ray photon loses energy during this process, the process is referred to as an *inelastic scattering event*. During such an event, the *phase* of the X-ray photon is changed in a random way, so that the photon no longer carries phase sensitive (i.e., diffraction) information. Compton modified radiation is thus useless from a diffraction point of view, but it does contribute to the signal in an X-ray detector. Photons which are scattered through the normal "Thomson" process do not undergo a random phase change, but have their phases modified by half a wavelength (phase shift of π). Thomson scattering is also known as *coherent* scattering.

12.1.2 Scattering by a single atom

When an X-ray beam is incident upon an atom with atomic number Z, each of its electrons will scatter the X-ray photons according to the Thomson equation. In addition, some of the X-ray intensity will be scattered *incoherently*, or via the Compton process. In this section, we will only regard the coherent scattering of X-rays by a single atom.

In the forward direction, $\theta = 0$, each of the Z electrons will scatter the beam with an identical phase change π. Since there is no difference between

the path lengths of the X-rays scattered in this direction (see Fig. 12.2(a)), there is also no destructive interference, and the total scattering in the forward direction is equal to Z times that of a single electron.

In all other directions, $\theta \neq 0$, there will be some path length difference between X-rays scattered by the different electrons and the total scattered intensity will decrease from the level of the forward scattered beam (see Fig. 12.2(b)). The exact mathematical theory for scattering from a single atom is described in some detail in Chapter 21. For now, it is sufficient to say that it involves an integral of the electron wave-function (multiplied by an appropriate quantum mechanical operator) over the entire volume of the atom. These calculations have been done for all atoms and the results are tabulated in the *International Tables for Crystallography*. From the mathematical treatment, one finds that the important variable governing the diffraction process is the ratio of the sine of half the diffraction angle to the wavelength, i.e., $\sin\theta/\lambda$. One defines the *atomic scattering factor*, f for a given angle θ and wavelength λ as the ratio of the amplitude scattered by the entire atom to the amplitude scattered in the same direction by a single electron. The atomic scattering factor is thus a function of the variable, $\sin\theta/\lambda$. The atomic scattering factors for Cu and Au are shown in Fig. 12.3. Note that the value for $\theta = 0$ is

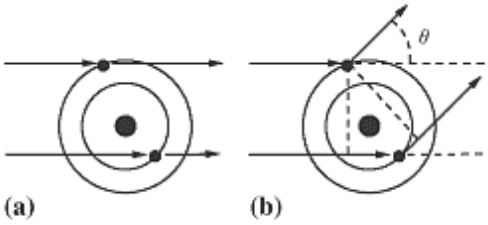

Fig. 12.2. (a) Forward scattering and (b) scattering at an angle θ. Note that there is no path length difference for forward scattering.

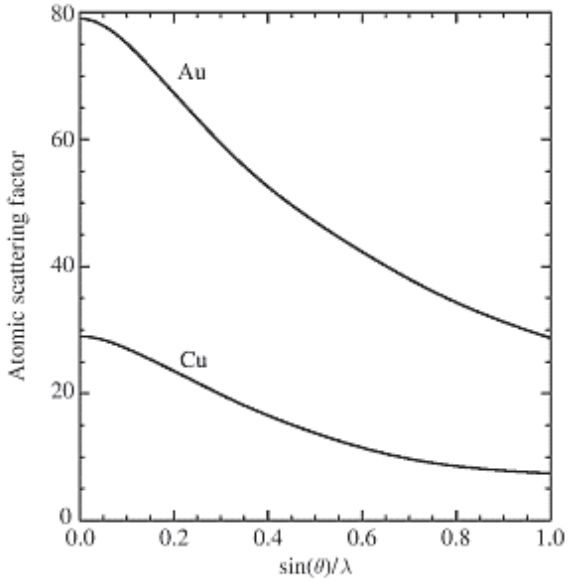

Fig. 12.3. Atomic scattering factors for copper and gold as a function of $\sin\theta/\lambda$.

indeed equal to the atomic number, and that the curve decreases rapidly with increasing scattering angle or decreasing wavelength.

Most tables list the atomic scattering factors in terms of curve fitting parameters. The curves represented in Fig. 12.3 are fitted with a sum of either three or four exponential functions. The scattering factor for a particular value of $\sin\theta/\lambda$ can then be computed using the following equation:

$$f(s) = Z - 41.782\,14 \times s^2 \times \sum_{i=1}^{N} a_i e^{-b_i s^2} \tag{12.3}$$

where $s = \sin\theta/\lambda$. The number of terms in the summation, N, is either 3 or 4. Table 12.1 lists the values of the coefficients a_i and b_i for all the elements in the periodic table. The elements that have a + in front of their atomic number use four terms in the expansion, the others use three terms. The numbers are the result of computations by Doyle & Turner (Doyle and Turner, 1968) and Smith & Burge (Smith and Burge, 1962). Note that the equation assumes that the wavelength is expressed in angstroms.

This table can be used in the following way: suppose one wants to compute the contribution of a single tungsten atom to diffraction of copper Kα radiation from the (222) plane of a body-centered cubic crystal with lattice parameter $a = 3.1653$Å.[1] We need to evaluate the scattering parameter s for this particular situation. From the Bragg equation we know that:

$$s = \frac{\sin\theta}{\lambda} = \frac{1}{2d_{hkl}}.$$

The value for d_{222} in a cubic crystal is easily found using:

$$d_{hkl} = \frac{a}{\sqrt{h^2 + k^2 + l^2}}$$

from which we find $d_{222} = 3.1653/\sqrt{12} = 0.9137$Å. The scattering parameter s is then equal to 0.5472 Å^{-1}. Substitution of this value, and the parameters for a_j and b_j for tungsten, into the atomic scattering factor equation results in:

$$\begin{aligned} f_W(0.5472) &= 74 - 41.78214 \times (0.5472)^2 \times \left[5.709e^{-28.782(0.5472)^2} + \right. \\ &\qquad \left. 4.677e^{-5.084(0.5472)^2} + 2.019e^{-0.572(0.5472)^2}\right] \\ &= 74 - 34.0642 \\ &= 39.9358. \end{aligned}$$

[1] Note that we work in angstroms instead of nanometers, since the values in Table 12.1 are listed in angstrom units.

Table 12.1. Atomic scattering parameters for all elements $Z = 1-98$: Doyle & Turner parameters have a + in front of the atomic number, the others are Smith & Burge parameters. This table assumes that s is expressed in $Å^{-1}$; if s is expressed in nm^{-1}, then all entries must be multiplied by 0.01.

Name	Z	a_1	b_1	a_2	b_2	a_3	b_3	a_4	b_4
Ac	89	6.278	28.323	5.195	4.949	2.321	0.557	—	—
Ag	+47	2.036	61.497	3.272	11.824	2.511	2.846	0.837	0.327
Al	+13	2.276	72.322	2.428	19.773	0.858	3.080	0.317	0.408
Am	95	6.378	29.156	5.495	5.102	2.495	0.565	—	—
Ar	+18	1.274	26.682	2.190	8.813	0.793	2.219	0.326	0.307
As	+33	2.399	45.718	2.790	12.817	1.529	2.280	0.594	0.328
At	85	6.133	28.047	5.031	4.957	2.239	0.558	—	—
Au	+79	2.388	42.866	4.226	9.743	2.689	2.264	1.255	0.307
B	+05	0.945	46.444	1.312	14.178	0.419	3.223	0.116	0.377
Ba	+56	7.821	117.657	6.004	18.778	3.280	3.263	1.103	0.376
Be	+04	1.250	60.804	1.334	18.591	0.360	3.653	0.106	0.416
Bi	+83	3.841	50.261	4.679	11.999	3.192	2.560	1.363	0.318
Bk	97	6.502	28.375	5.478	4.975	2.510	0.561	—	—
Br	+35	2.166	33.899	2.904	10.497	1.395	2.041	0.589	0.307
C	+06	0.731	36.995	1.195	11.297	0.456	2.814	0.125	0.346
Ca	+20	4.470	99.523	2.971	22.696	1.970	4.195	0.482	0.417
Cd	+48	2.574	55.675	3.259	11.838	2.547	2.784	0.838	0.322
Ce	58	5.007	28.283	3.980	5.183	1.678	0.589	—	—
Cf	98	6.548	28.461	5.526	4.965	2.520	0.557	—	—
Cl	+17	1.452	30.935	2.292	9.980	0.787	2.234	0.322	0.323
Cm	96	6.460	28.396	5.469	4.970	2.471	0.554	—	—
Co	+27	2.367	61.431	2.236	14.180	1.724	2.725	0.515	0.344
Cr	+24	2.307	78.405	2.334	15.785	1.823	3.157	0.490	0.364
Cs	+55	6.062	155.837	5.986	19.695	3.303	3.335	1.096	0.379
Cu	+29	1.579	62.940	1.820	12.453	1.658	2.504	0.532	0.333
Dy	66	5.332	28.888	4.370	5.198	1.863	0.581	—	—
Er	68	5.436	28.655	4.437	5.117	1.891	0.577	—	—
Eu	+63	6.267	100.298	4.844	16.066	3.202	2.980	1.200	0.367
F	+09	0.387	20.239	0.811	6.609	0.475	1.931	0.146	0.279
Fe	+26	2.544	64.424	2.343	14.880	1.759	2.854	0.506	0.350
Fr	87	6.201	28.200	5.121	4.954	2.275	0.556	—	—
Ga	+31	2.321	65.602	2.486	15.458	1.688	2.581	0.599	0.351
Gd	64	5.225	29.158	4.314	5.259	1.827	0.586	—	—
Ge	+32	2.447	55.893	2.702	14.393	1.616	2.446	0.601	0.342
H	01	0.202	30.868	0.244	8.544	0.082	1.273	—	—
He	+02	0.091	18.183	0.181	6.212	0.110	1.803	0.036	0.284
Hf	72	5.588	29.001	4.619	5.164	1.997	0.579	—	—
Hg	+80	2.682	42.822	4.241	9.856	2.755	2.295	1.270	0.307
Ho	67	5.376	28.773	4.403	5.174	1.884	0.582	—	—
I	+53	3.473	39.441	4.060	11.816	2.522	2.415	0.840	0.298
In	+49	3.153	66.649	3.557	14.449	2.818	2.976	0.884	0.335
Ir	77	5.754	29.159	4.851	5.152	2.096	0.570	—	—
K	+19	3.951	137.075	2.545	22.402	1.980	4.532	0.482	0.434
Kr	+36	2.034	29.999	2.927	9.598	1.342	1.952	0.589	0.299
La	57	4.940	28.716	3.968	5.245	1.663	0.594	—	—
Li	+03	1.611	107.638	1.246	30.480	0.326	4.533	0.099	0.495
Lu	71	5.553	28.907	4.580	5.160	1.969	0.577	—	—

Table 12.1. (cont.).

Name	Z	a_1	b_1	a_2	b_2	a_3	b_3	a_4	b_4
Mg	+12	2.268	73.670	1.803	20.175	0.839	3.013	0.289	0.405
Mn	+25	2.747	67.786	2.456	15.674	1.792	3.000	0.498	0.357
Mo	+42	3.120	72.464	3.906	14.642	2.361	3.237	0.850	0.366
N	+07	0.572	28.847	1.043	9.054	0.465	2.421	0.131	0.317
Na	+11	2.241	108.004	1.333	24.505	0.907	3.391	0.286	0.435
Nb	41	4.237	27.415	3.105	5.074	1.234	0.593	—	—
Nd	60	5.151	28.304	4.075	5.073	1.683	0.571	—	—
Ne	+10	0.303	17.640	0.720	5.860	0.475	1.762	0.153	0.266
Ni	+28	2.210	58.727	2.134	13.553	1.689	2.609	0.524	0.339
Np	93	6.323	29.142	5.414	5.096	2.453	0.568	—	—
O	+08	0.455	23.780	0.917	7.622	0.472	2.144	0.138	0.296
Os	76	5.750	28.933	4.773	5.139	2.079	0.573	—	—
P	+15	1.888	44.876	2.469	13.538	0.805	2.642	0.320	0.361
Pa	91	6.306	28.688	5.303	5.026	2.386	0.561	—	—
Pb	+82	3.510	52.914	4.552	11.884	3.154	2.571	1.359	0.321
Pd	46	4.436	28.670	3.454	5.269	1.383	0.595	—	—
Pm	61	5.201	28.079	4.094	5.081	1.719	0.576	—	—
Po	84	6.070	28.075	4.997	4.999	2.232	0.563	—	—
Pr	59	5.085	28.588	4.043	5.143	1.684	0.581	—	—
Pt	78	5.803	29.016	4.870	5.150	2.127	0.572	—	—
Pu	94	6.415	28.836	5.419	5.022	2.449	0.561	—	—
Ra	88	6.215	28.382	5.170	5.002	2.316	0.562	—	—
Rb	+37	4.776	140.782	3.859	18.991	2.234	3.701	0.868	0.419
Re	75	5.695	28.968	4.740	5.156	2.064	0.575	—	—
Rh	45	4.431	27.911	3.343	5.153	1.345	0.592	—	—
Rn	+86	4.078	38.406	4.978	11.020	3.096	2.355	1.326	0.299
Ru	44	4.358	27.881	3.298	5.179	1.323	0.594	—	—
S	+16	1.659	36.650	2.386	11.488	0.790	2.469	0.321	0.340
Sb	+51	3.564	50.487	3.844	13.316	2.687	2.691	0.864	0.316
Sc	+21	3.966	88.960	2.917	20.606	1.925	3.856	0.480	0.399
Se	+34	2.298	38.830	2.854	11.536	1.456	2.146	0.590	0.316
Si	+14	2.129	57.775	2.533	16.476	0.835	2.880	0.322	0.386
Sm	62	5.255	28.016	4.113	5.037	1.743	0.577	—	—
Sn	+50	3.450	59.104	3.735	14.179	2.118	2.855	0.877	0.327
Sr	+38	5.848	104.972	4.003	19.367	2.342	3.737	0.880	0.414
Ta	73	5.659	28.807	4.630	5.114	2.014	0.578	—	—
Tb	65	5.272	29.046	4.347	5.226	1.844	0.585	—	—
Tc	43	4.318	28.246	3.270	5.148	1.287	0.590	—	—
Te	52	4.785	27.999	3.688	5.083	1.500	0.581	—	—
Th	90	6.264	28.651	5.263	5.030	2.367	0.563	—	—
Ti	+22	3.565	81.982	2.818	19.049	1.893	3.590	0.483	0.386
Tl	81	5.932	29.086	4.972	5.126	2.195	0.572	—	—
Tm	69	5.441	29.149	4.510	5.264	1.956	0.590	—	—
U	+92	6.767	85.951	6.729	15.642	4.014	2.936	1.561	0.335
V	+23	3.245	76.379	2.698	17.726	1.860	3.363	0.486	0.374
W	74	5.709	28.782	4.677	5.084	2.019	0.572	—	—
Xe	+54	3.366	35.509	4.147	11.117	2.443	2.294	0.829	0.289
Y	39	4.129	27.548	3.012	5.088	1.179	0.591	—	—
Yb	70	5.529	28.927	4.533	5.144	1.945	0.578	—	—
Zn	+30	1.942	54.162	1.950	12.518	1.619	2.416	0.543	0.330
Zr	40	4.105	28.492	3.144	5.277	1.229	0.601	—	—

Note that this number is independent of the wave length of the X-rays being used since the number $1/2d_{hkl}$ is independent of the wave length.

12.1.3 Scattering by a single unit cell

The scattering of X-rays due to a complete unit cell can be computed by taking into account the *relative* positions of all the atoms in the unit cell. We know that scattering from electrons belonging to the same atom can give rise to destructive interference because of the relative positions of the electrons inside the electron cloud. A similar thing happens for scattering from a unit cell. Consider the simple example shown in Fig. 12.4. Rays 1 and 2 are diffracted from the planes (hkl) if they satisfy the Bragg equation, which means that the path length difference between the two waves must be equal to the wave length λ. Suppose that the interplanar spacing d is equal to one of the lattice parameters, say a. In that case we would be talking about the (100) planes. If we add an atom to the unit cell, say at position $(1/2, 0, 0)$, exactly in between the atoms at O and O', then X-rays will also be scattered by this atom. The diffracted waves 1′ and 2′ are in phase (i.e., path length difference equal to λ), and from the drawing it is easy to see that the pathlength difference between 1′ and 3′ (and also between 2′ and 3′) is equal to *half of the wave length*, $\lambda/2$. This means that the waves are out-of-phase, which means that they will cancel each other out, despite the fact that geometrically the Bragg equation for the planes (100) is satisfied! The additional atom is located on the (200) plane. If we were to construct the diffraction condition for this plane, then we would find that diffracted beams from the (200) planes, with diffraction angle θ different from that for the (100) planes, are in-phase, which means that the (200) planes *will* give rise to a diffracted beam.

This example illustrates that diffraction from a certain set of planes (hkl) not only depends on the particular orientation of the incoming beam with respect to the plane, but also on the particular position of atoms within the unit cell with respect to the plane. One can show graphically, that the phase difference between waves 1′ and 3′ does not depend on the position of the extra atom within the (200) plane; i.e., moving the atom within the plane does not change the destructive interference between the two beams. We thus

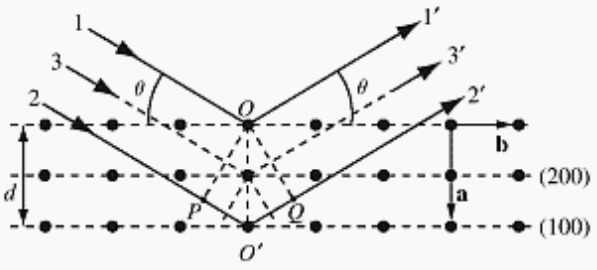

Fig. 12.4. The waves diffracted from the (100) planes interfere destructively when an atom is added in the (200) plane.

conclude that the only thing that matters is the distance between the extra atom and the (100) plane. This distance can be expressed by the projection of the position vector $\mathbf{r}$ of the atom onto the normal to the plane (100). We have seen in Chapter 6 that the plane normal is given by $\mathbf{g}_{100}$, and the projection of $\mathbf{r}$ onto $\mathbf{g}_{100}$ is equal to the dot-product $\mathbf{g}_{100} \cdot \mathbf{r}$. If we take the extra atom to be at the position $(1/2, 0, 0)$, then this dot-product becomes equal to:

$$\mathbf{g}_{100} \cdot \mathbf{r} = 1\mathbf{a}^* . \frac{1}{2}\mathbf{a} = \frac{1}{2}.$$

Here we have used the definition of the reciprocal lattice vectors. We can translate the projection of $\mathbf{r}$ onto the plane normal into a phase difference by multiplying the dot-product with 2π. This leads to a phase difference of π, since:

$$2\pi \mathbf{g}_{100} \cdot \mathbf{r} = \pi,$$

and, therefore, waves scattered by the extra atom and the (100) planes are out-of-phase. If the extra atom is at position $(1/2, y, z)$, i.e., still in the (200) plane, then the phase difference becomes:

$$2\pi \mathbf{g}_{100} \cdot \mathbf{r} = 2\pi \mathbf{a}^* \cdot \frac{1}{2}\mathbf{a} + 2\pi \mathbf{a}^* \cdot y\mathbf{b} + 2\pi \mathbf{a}^* \cdot z\mathbf{c} = \pi,$$

where again we have used the properties of the reciprocal basis vectors. We find that adding an atom to a unit cell affects the diffraction from all lattice planes (hkl) in a way determined by the phase difference $2\pi \mathbf{g}_{hkl} \cdot \mathbf{r}$, where $\mathbf{r}$ is the position vector of the atom with respect to the direct basis vectors. In general, the phase difference is expressed by:

$$\boxed{\phi = 2\pi \mathbf{g}_{hkl} \cdot \mathbf{r} = 2\pi(hx + ky + lz).} \tag{12.4}$$

In the previous section, we have seen how strongly a single atom scatters X-rays in a particular direction. In the present section, we have determined the relative phase for scattering from two atoms. We can combine these two numbers, amplitude and phase, into a single complex number:

$$f(s)e^{i\phi} = f(\frac{\sin\theta}{\lambda})e^{2\pi i \mathbf{g}_{hkl} \cdot \mathbf{r}}. \tag{12.5}$$

This expression states how an atom at position $\mathbf{r}$ contributes to diffraction of X-rays of wavelength λ from the plane (hkl). Scattering from a complete unit cell is then described by adding together these factors for all atoms in the unit cell.

12.2 The structure factor

The quantity describing scattering from a complete unit cell is known as the *structure factor*, and is represented by the symbol F_{hkl}. The formal definition of the structure factor is:

$$F_{hkl} = \sum_{j=1}^{N} f_j\left(\frac{\sin\theta_{hkl}}{\lambda}\right) e^{2\pi i \mathbf{g}_{hkl}\cdot\mathbf{r}_j} = \sum_{j=1}^{N} f_j\left(\frac{\sin\theta_{hkl}}{\lambda}\right) e^{2\pi i(hx_j+ky_j+lz_j)}. \tag{12.6}$$

with N the number of atoms in the unit cell. The intensity in the diffracted beam from the planes (hkl) is proportional to the *modulus squared of the structure factor*:

$$I_{hkl} = |F_{hkl}|^2 = F_{hkl}F_{hkl}^*, \tag{12.7}$$

where the asterisk indicates complex conjugation.

This structure factor also has a geometrical interpretation: scattering from each atom is represented by a complex number $fe^{i\phi}$. We know that a complex number can be represented by a vector in the complex plane, as shown in Fig. 12.5(a), which shows the complex number $2e^{i\pi/3}$. Scattering from an individual atom is represented by such a number or vector, and, therefore, the addition of all complex numbers in the structure factor is equivalent to vector addition of all the corresponding vectors in the complex plane (Fig. 12.5(b)). This is known as an *Argand diagram*. If the positions of atoms in the unit cell are such that for a particular set of planes (hkl) the total sum of complex vectors ends up in the origin, then there will be no diffracted beam for that particular plane, *even when the Bragg condition is satisfied.* This is known as an *extinction*. There are several possible reasons for extinctions to occur, and we will discuss the most important ones in the following sections.

12.2.1 Lattice centering and the structure factor

We have seen in the previous chapter that the geometry of the diffraction process is completely determined by the shape and dimensions of the unit

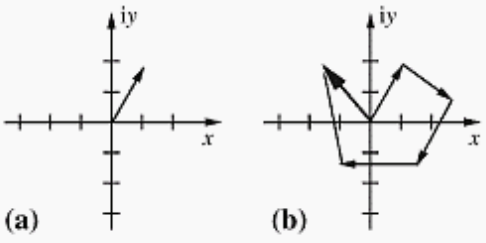

Fig. 12.5. (a) Graphical representation of the complex number $2e^{i\pi/3}$; (b) The scattering from all atoms in a unit cell is computed by adding all corresponding vectors; the thicker vector is equal to the structure factor. The square of the length of this vector is proportional to the total diffracted intensity.

cell. The structure factor is independent of the lattice parameters. Note that this is the case because of the particular definition we use for the reciprocal lattice vectors. In the following subsections, we will look at the four possible types of centering (P, C, I, and F) and determine the extinctions for each of them.

12.2.1.1 Primitive lattice

A primitive lattice is characterized by the absence of any centering vectors. This means that for the most general atom position $\mathbf{r} = (x, y, z)$ (general in the sense that the atom does not lie on a symmetry element of the structure) *there is no equivalent atom located at any of the positions* $\mathbf{r}+\mathbf{A}$, $\mathbf{r}+\mathbf{B}$, $\mathbf{r}+\mathbf{C}$, or $\mathbf{r}+\mathbf{I}$ (using the notation from Chapter 3). For a primitive structure with only one atom in the unit cell, say at $\mathbf{r} = (0, 0, 0)$, we find:

$$F_{hkl} = \sum_{j=1}^{1} f_j e^{2\pi i(h0+k0+l0)} = f,$$

and, therefore, the diffracted intensity is proportional to $I_{hkl} = f^2$. Remember that the value of f does depend on the particular lattice plane (hkl). In other words, for a primitive lattice there are no extinctions; all lattice planes give rise to a diffracted beam.

12.2.1.2 C-centered lattice

A C-centered lattice is characterized by the fact that, for every atom at position $\mathbf{r}$, there is an *identical* atom at position $\mathbf{r}+\mathbf{C}$. The structure factor for this situation (for $\mathbf{r} = (0, 0, 0)$) is given by:

$$F_{hkl} = \sum_{j=1}^{2} f_j e^{2\pi i(hx_j+ky_j+lz_j)} = f(1+e^{\pi i(h+k)}).$$

Using the properties of exponentials and Euler's formula we can rewrite this as:

$$\begin{aligned} F_{hkl} &= f e^{\frac{\pi}{2}i(h+k)}\left(e^{-\frac{\pi}{2}i(h+k)}+e^{\frac{\pi}{2}i(h+k)}\right); \\ &= 2f e^{\frac{\pi}{2}i(h+k)}\cos\frac{\pi}{2}(h+k). \end{aligned}$$

The intensity in the diffracted beams is then proportional to:

$$\begin{aligned} |F_{hkl}|^2 &= \left(2f e^{\frac{\pi}{2}i(h+k)}\cos\frac{\pi}{2}(h+k)\right)\left(2f e^{-\frac{\pi}{2}i(h+k)}\cos\frac{\pi}{2}(h+k)\right); \\ &= 4f^2\cos^2\frac{\pi}{2}(h+k). \end{aligned} \tag{12.8}$$

This intensity vanishes whenever the cosine becomes zero, and this happens whenever $h+k = 2n+1$. We conclude that for a C-centered lattice all

diffracted beams with $h+k=$ odd, will vanish. These extinctions are called *systematic absences* or *systematic extinctions*. Note again that this is true independent of the shape and dimensions of the unit cell; in particular, it is true for the *mC* and *oC* Bravais lattices.

12.2.1.3 Body-centered lattice

The body-centered lattice is characterized by the presence of an *identical* atom at position $\mathbf{r}+\mathbf{I}$ for every atom at position $\mathbf{r}$. The structure factor is thus written as:

$$F_{hkl} = f\left(1+\mathrm{e}^{\pi\mathrm{i}(h+k+l)}\right).$$

and, using the same mathematical steps as before, we find for the intensity:

$$I_{hkl} = 4f^2\cos^2\frac{\pi}{2}(h+k+l), \tag{12.9}$$

from which we derive that for the body-centered lattices, all reflections with $h+k+l=$ odd will vanish. This is in particular true for the *oI*, *tI*, and *cI* Bravais lattices.

12.2.1.4 Face-centered lattice

The face-centered lattice is characterized by the simultaneous presence of three centering vectors, **A**, **B**, and **C**. The structure factor thus contains four terms:

$$F_{hkl} = f\left(1+\mathrm{e}^{\pi\mathrm{i}(h+k)}+\mathrm{e}^{\pi\mathrm{i}(h+l)}+\mathrm{e}^{\pi\mathrm{i}(k+l)}\right).$$

To compute the intensity we can now proceed in three different ways: (1) we multiply this expression with its complex conjugate and work out all the terms (a tedious task); (2) we attempt to rewrite the expression as the product of trigonometric functions (product, because it is easy to determine when a product will be zero); or (3) we use the fact that $\mathrm{e}^{\pi\mathrm{i}}=-1$. First we follow the second method. Let us take a closer look at the following product:

$$\left(1+\mathrm{e}^{\pi\mathrm{i}(h+k)}\right)\left(1+\mathrm{e}^{\pi\mathrm{i}(h+l)}\right) = 1+\mathrm{e}^{\pi\mathrm{i}(h+k)}+\mathrm{e}^{\pi\mathrm{i}(h+l)}+\mathrm{e}^{\pi\mathrm{i}(2h+k+l)}.$$

This expression is equal to the structure factor above, except for the factor $2h$ in the third exponential. However, from Euler's formula we know that:

$$\mathrm{e}^{2\pi\mathrm{i}h} = \cos 2\pi h + \mathrm{i}\sin 2\pi h = 1,$$

for all integers h. We can thus replace the structure factor by:

$$\begin{aligned} F_{hkl} &= f\left(1+\mathrm{e}^{\pi\mathrm{i}(h+k)}\right)\left(1+\mathrm{e}^{\pi\mathrm{i}(h+l)}\right); \\ &= 4f\mathrm{e}^{\frac{\pi}{2}\mathrm{i}(h+k)}\cos\frac{\pi}{2}(h+k)\mathrm{e}^{\frac{\pi}{2}\mathrm{i}(h+l)}\cos\frac{\pi}{2}(h+l), \end{aligned}$$

Table 12.2. Comparison of the extinctions in the three cubic Bravais lattices.

(hkl)	$h^2+k^2+l^2$	cP	cI	cF
(100)	1	f^2	0	0
(110)	2	f^2	$4f^2$	0
(111)	3	f^2	0	$16f^2$
(200)	4	f^2	$4f^2$	$16f^2$
(210)	5	f^2	0	0
(211)	6	f^2	$4f^2$	0
(220)	8	f^2	$4f^2$	$16f^2$
(221)	9	f^2	0	0
(300)	9	f^2	0	0
(310)	10	f^2	$4f^2$	0
(311)	11	f^2	0	$16f^2$
(222)	12	f^2	$4f^2$	$16f^2$
(320)	13	f^2	0	0
(321)	14	f^2	$4f^2$	0
(400)	16	f^2	$4f^2$	$16f^2$
(322)	17	f^2	0	0
(410)	17	f^2	0	0

from which we find for the intensity

$$I_{hkl} = 16f^2 \cos^2 \frac{\pi}{2}(h+k) \cos^2 \frac{\pi}{2}(h+l). \tag{12.10}$$

This expression is equal to zero whenever the Miller indices h, k, and l have different parity; in other words, for a face-centered lattice only reflections with all Miller indices even or all odd will be present. Mixed reflections will be absent. For all allowed reflections the cosine functions are equal to 1, and we find $I_{hkl} = 16f^2$.

We can also follow the third method, which goes as follows: we use the following property of the exponential function:

$$e^{\pi i(h+k)} = \left(e^{\pi i}\right)^{h+k} = (-1)^{h+k},$$

which allows us to rewrite the structure factor as

$$F_{hkl} = f\left(1+(-1)^{h+k}+(-1)^{h+l}+(-1)^{k+l}\right). \tag{12.11}$$

For mixed indices, two of these factors are equal to -1, and two are equal to $+1$, so that their sum vanishes and $F_{hkl} = 0$. For indices of equal parity, all terms are equal to $+1$ and hence $F_{hkl} = 4f$, or $I_{hkl} = 16f^2$. The results for all different centering variants of the cubic lattice are summarized in Table 12.2. This table can be compared with Table 11.3 on page 276, which lists the Bragg angles for a number of planes in face-centered cubic copper; only a few

of the planes will actually give rise to a diffracted beam due to centering extinctions.

12.2.2 Symmetry and the structure factor

In the previous section we have seen how lattice centering causes systematic absences. Symmetry elements can also give rise to extinctions. Let us consider three examples:

(i) **Inversion symmetry**: An inversion center is characterized by the fact that for every atom at position $\mathbf{r}$ there is an equivalent atom at position $-\mathbf{r}$. If we have a unit cell with N atoms, then we can split the structure factor for that cell in two terms:

$$\begin{aligned} F_{hkl} &= \sum_{j=1}^{N} f_j e^{2\pi i \mathbf{g}\cdot\mathbf{r}_j}; \\ &= \sum_{j=1}^{N/2} f_j \left(e^{2\pi i \mathbf{g}\cdot\mathbf{r}_j} + e^{-2\pi i \mathbf{g}\cdot\mathbf{r}_j}\right); \\ &= 2\sum_{j=1}^{N/2} f_j \cos\left(2\pi \mathbf{g}\cdot\mathbf{r}_j\right). \end{aligned}$$

The last summation is a sum of *real* numbers, and therefore we conclude that the structure factor for a unit cell with inversion symmetry is always a real number.

(ii) **Screw axis symmetry**: A screw axis can be represented by a 4×4 transformation matrix which indicates how atom coordinates of equivalent atoms are related to one another. As an example, we consider the presence of a 4_1 screw axis, parallel to the c-axis and going through the origin of the unit cell. For every atom at position $\mathbf{r} = (x, y, z)$, there are three additional equivalent atoms, at positions $(-y, x, z+1/4)$, $(-x, -y, z+1/2)$, and $(y, -x, z+3/4)$. The structure factor can thus be rewritten as:

$$\begin{aligned} F_{hkl} = \sum_{j=1}^{N/4} f_j \Big[& e^{2\pi i(hx_j+ky_j+lz_j)} + e^{2\pi i(-hy_j+kx_j+l(z_j+\frac{1}{4})} \\ & + e^{2\pi i(-hx_j-ky_j+l(z_j+\frac{1}{2})} + e^{2\pi i(hy_j-kx_j+l(z_j+\frac{3}{4})} \Big]. \end{aligned}$$

This equation can be simplified substantially if we only consider reflections of the type $(00l)$. In that case we can write:

$$F_{00l} = \left(\sum_{s=0}^{3} e^{\pi i \frac{sl}{2}}\right) \sum_{j=1}^{N/4} f_j e^{2\pi i l z_j}.$$

Table 12.3. Systematic absences for screw axes parallel to the **c** direction.

Screw axis	$\lvert\tau\rvert$	extinction for
2_1	$c/2$	$l = 2n+1$
$3_1, 3_2$	$\pm c/3$	$l \neq 3n$
$4_1, 4_3$	$\pm c/4$	$l \neq 4n$
4_2	$c/2$	$l = 2n+1$
$6_1, 6_5$	$\pm c/6$	$l \neq 6n$
$6_2, 6_4$	$\pm c/3$	$l \neq 3n$
6_3	$c/2$	$l = 2n+1$

The first factor is a simple finite geometric series and it is easy to show that it can be rewritten as:

$$\sum_{s=0}^{3} \mathrm{e}^{\pi \mathrm{i} \frac{sl}{2}} = \frac{1-\mathrm{e}^{2\pi \mathrm{i} l}}{1-\mathrm{e}^{\pi \mathrm{i} \frac{l}{2}}}.$$

The numerator of this expression is always equal to zero; we have to be careful with the denominator, however, because the ratio 0/0 is not defined. The denominator becomes equal to zero whenever $l = 4n$, with n an integer. The value of the ratio is then determined by the de l'Hopital rule, which states that the value for l approaching $4n$ is equal to the ratio of the derivatives of nominator and denominator, evaluated at $l = 4n$. In mathematical terms this means:

$$\begin{aligned} \lim_{l \to 4n} \frac{1-\mathrm{e}^{2\pi \mathrm{i} l}}{1-\mathrm{e}^{\pi \mathrm{i} \frac{l}{2}}} &= \lim_{l \to 4n} \frac{-2\pi \mathrm{i} \mathrm{e}^{2\pi \mathrm{i} l}}{-\frac{\pi \mathrm{i}}{2} \mathrm{e}^{\pi \mathrm{i} \frac{l}{2}}}; \\ &= \lim_{l \to 4n} 4\mathrm{e}^{\pi \mathrm{i} \frac{3l}{2}}; \\ &= 4\mathrm{e}^{6\pi \mathrm{i} n} = 4. \end{aligned}$$

Summarizing, we find that the reflections of the type $(00l)$, with $l \neq 4n$ are absent in the presence of a screw axis of the type 4_1 parallel to the c-axis. One can derive similar extinction conditions for all other screw axes and the results are summarized in Table 12.3.

(iii) **Glide plane symmetry**: For a glide plane we can apply a similar method to determine which reflections will be absent. Let us consider an n glide plane, parallel to the (001) plane, going through the origin, with translation vector $\tau = (1/2, 1/2, 0)$. For each atom at position (x, y, z) there is an equivalent atom at position $(x+1/2, y+1/2, \bar{z})$. The structure factor can thus be written as:

$$F_{hkl} = \sum_{j=1}^{N/2} f_j \left(\mathrm{e}^{2\pi \mathrm{i}(hx_j + ky_j + lz_j)} + \mathrm{e}^{2\pi \mathrm{i}(hx_j + \frac{h}{2} + ky_j + \frac{k}{2} - lz_j)} \right);$$

Table 12.4. Systematic absences in the ($hk0$) reflections for glide planes parallel to the (001) plane.

glide type	$\lvert\boldsymbol{\tau}\rvert$	extinction for
a	$\frac{a}{2}$	$h = 2n+1$
b	$\frac{b}{2}$	$k = 2n+1$
n	$\frac{a+b}{2}$	$h+k = 2n+1$
d	$\frac{a\pm b}{4}$	$h+k = 4n+2$ with $h = 2n$ and $k = 2n$

$$= \sum_{j=1}^{N/2} f_j e^{2\pi i(hx_j+ky_j)} \left(e^{2\pi i l z_j} + e^{2\pi i(\frac{h+k}{2} - l z_j)}\right)$$

For reflections of the type ($hk0$) we find:

$$F_{hk0} = \sum_{j=1}^{N/2} f_j e^{2\pi i(hx_j+ky_j)} \left(1 + e^{2\pi i(\frac{h+k}{2})}\right);$$

$$= 2e^{\pi i \frac{h+k}{2}} \cos\pi\left(\frac{h+k}{2}\right) \sum_{j=1}^{N/2} f_j e^{2\pi i(hx_j+ky_j)},$$

and therefore the structure factor becomes zero whenever $h+k = 2n+1$. Summarizing, we find that the reflections of the type ($hk0$), with $h+k = 2n+1$, are absent in the presence of a glide plane parallel to (001), going through the origin, with glide vector $\boldsymbol{\tau} = (1/2, 1/2, 0)$. One can derive similar extinction conditions for all other glide planes and the results for glide planes parallel to (001) are summarized in Table 12.4.

This concludes the discussion of the effect of symmetry elements on the structure factor. As a final remark we should mention that diffraction from a given crystal structure will always have an intrinsic symmetry. This is caused by the following observation: since we can only measure intensities, and not phases, we cannot distinguish between the (hkl) plane and the ($\bar{h}\bar{k}\bar{l}$) plane. For structures without inversion symmetry, the structure factor for the (hkl) plane is equal to the complex conjugate of that of the ($\bar{h}\bar{k}\bar{l}$) plane, or:

$$F_{hkl} = F^*_{\bar{h}\bar{k}\bar{l}}.$$

Therefore, we also have:

$$F^*_{hkl} = F_{\bar{h}\bar{k}\bar{l}}.$$

Combining these relations we have:

$$I_{hkl} = F_{hkl}F^*_{hkl} = F_{\bar{h}\bar{k}\bar{l}}F^*_{\bar{h}\bar{k}\bar{l}} = I_{\bar{h}\bar{k}\bar{l}}. \tag{12.12}$$

Therefore, an X-ray diffraction data set will *always* display a center of symmetry, even when the crystal structure does not. This is known as *Friedel's law*. As a consequence, the point group symmetry of a diffraction data set must belong to one of the 11 *Laue classes* described in section 9.2.10.1 on page 214.

12.2.3 Systematic absences and the International Tables for Crystallography

In Chapter 10 we described how the *International Tables for Crystallography* list all 230 space groups. In particular, we showed a portion of the actual entries for space groups **Cmm2** (C_{2v}^{11}) and **Pmna** (D_{2h}^{7}) in Figs. 10.11 and 10.12. Under the entry "**Positions**", which lists the Wyckoff positions and the coordinates of the equivalent positions for general and special sites, we find information about the "reflection conditions," i.e., the conditions that need to be satisfied by the Miller indices h, k, and l in order to have a diffracted beam (non-zero structure factor). Note that these conditions are the opposite of the extinction conditions.

Consider space group **Cmm2** (C_{2v}^{11}) as an example. The space group is C-centered, so that the extinction condition derived previously reads $h+k=2n+1$, i.e., the structure factor vanishes for all odd $h+k$. The International Tables then state the reflection condition $h+k=2n$, i.e., $h+k$ must be even to have a non-zero structure factor. The general condition is typically simplified for special combinations of the indices, such as $h00$ for which the reflection condition simplifies to $h=2n$. For the special positions all general reflection conditions apply, and sometimes there are additional conditions. For instance, for **Cmm2** (C_{2v}^{11}) we have for the $4c$ Wyckoff position the additional reflection condition $hkl : h=2n$. In other words, if we have a structure with space group **Cmm2** (C_{2v}^{11}), and with atoms only on the $4c$ site, then only planes for which h is even can give rise to a diffracted beam. Since we must also satisfy the general reflection condition $h+k=2n$, and h is even, we find that k must also be even.

For space group **Pmna** (D_{2h}^{7}), with a diagonal glide plane n normal to the **b** direction, we find the general reflection condition $h0l : h+l=2n$, similar to the derivation in the present chapter. For nearly all special positions, there is an additional condition: $hkl : h+l=2n$, i.e., the general condition is not only valid for $k=0$, but must be valid for all values of k. The exception is the $4h$ Wyckoff position, for which no extra conditions apply.

From these examples we see how the space group symmetry, which is a combination of lattice centering and point group symmetry, dictates which planes can give rise to a diffracted beam. Conversely, by studying a diffraction data set, we can determine which planes do not give rise to a diffracted beam, and from this information we can, in principle, determine to which space group the structure belongs. We will return to the topic of space group determination in the next chapter, when we talk about convergent beam electron diffraction.

12.2.4 Examples of structure factor calculations

In this section, we will carry out a few simple structure factor calculations for the CsCl structure, the NaCl structure, and the diamond structure. In later chapters, the reader will find additional examples of structure factor computations.

Example 1: CsCl. The unit cell of CsCl contains only two atoms, Cs in the origin and Cl at the center of the cell, so that the structure factor is given by:

$$F_{hkl} = f_{\mathrm{Cs}} + f_{\mathrm{Cl}}(-1)^{h+k+l}.$$

For the reflections with $h+k+l=2n$ we find that $F_{hkl} = f_{\mathrm{Cs}} + f_{\mathrm{Cl}}$; for all other reflections we have $F_{hkl} = f_{\mathrm{Cs}} - f_{\mathrm{Cl}}$. The observed intensities will hence be equal to:

$$\begin{aligned} I_{hkl} &= (f_{\mathrm{Cs}} + f_{\mathrm{Cl}})^2 \quad \text{for } h+k+l=2n; \\ I_{hkl} &= (f_{\mathrm{Cs}} - f_{\mathrm{Cl}})^2 \quad \text{for } h+k+l=2n+1. \end{aligned}$$

This means that we now have two sets of reflections: reflections with intensities proportional to the square of the *sum* of the atomic scattering factors, and reflections proportional to the square of the *difference* of the atomic scattering factors. The former reflections are known as *fundamental reflections*, the weaker ones as *superlattice reflections*.

If Cs and Cl were *randomly* distributed over the two sites of a body-centered cubic unit cell, then the atomic scattering factor for each site would be the average of those of the atoms, i.e., $f = (f_{\mathrm{Cs}} + f_{\mathrm{Cl}})/2$, and then the reflections with $h+k+l=2n+1$ would have zero intensity, as required for a body-centered cell. Any deviation from the random arrangement of the atoms results in a non-zero intensity for these reflections, and, therefore, the superlattice reflections give information on the *degree of order* in the material.

Example 2: NaCl. The sodium chloride structure can be regarded as two interpenetrating *fcc* lattices, one filled with Na and the other with Cl. The structure factor for each individual lattice is equal to that for a regular *fcc* lattice. The Cl lattice is shifted with respect to the Na lattice by a vector $\boldsymbol{\tau} = (1/2, 1/2, 1/2)$. This means that the total structure factor can be written as:

$$\begin{aligned} F_{hkl} = {} & f_{\mathrm{Na}}(1+(-1)^{h+k}+(-1)^{h+l}+(-1)^{k+l}) \\ & + f_{\mathrm{Cl}}\,\mathrm{e}^{\pi i(h+k+l)}(1+(-1)^{h+k}+(-1)^{h+l}+(-1)^{k+l}). \end{aligned}$$

Since $\mathrm{e}^{\pi i n} = (-1)^n$ we find:

$$F_{hkl} = (f_{\mathrm{Na}} + f_{\mathrm{Cl}}(-1)^{h+k+l})(1+(-1)^{h+k}+(-1)^{h+l}+(-1)^{k+l}).$$

The corresponding intensity is thus given by:

$$I_{hkl} = (f_{\mathrm{Na}} + f_{\mathrm{Cl}}(-1)^{h+k+l})^2 \times (1 + (-1)^{h+k} + (-1)^{h+l} + (-1)^{k+l})^2.$$

We already know from the *fcc* example that only reflections for which all indices have the same parity are allowed. In addition, the presence of the second *fcc* lattice introduces a new condition: if $h+k+l = 2n$, then the two atomic scattering factors must be added, if $h+k+l = 2n+1$ then they are subtracted. The intensities for NaCl are thus as follows:

$$I_{hkl} = 0 \quad \text{for } h,k,l \text{ different parity;}$$
$$I_{hkl} = 16(f_{\mathrm{Na}} + f_{\mathrm{Cl}})^2 \quad \text{for } h,k,l \text{ same parity and } h+k+l = 2n;$$
$$I_{hkl} = 16(f_{\mathrm{Na}} - f_{\mathrm{Cl}})^2 \quad \text{for } h,k,l \text{ same parity and } h+k+l = 2n+1.$$

Once again we find two different sets of reflections: fundamental reflections and superlattice reflections.

Example 3: Diamond. The diamond structure can also be regarded as two interpenetrating *fcc* lattices, but this time with translation vector $\boldsymbol{\tau} = (1/4, 1/4, 1/4)$. The structure factor thus becomes:

$$\begin{aligned} F_{hkl} = {} & f_{\mathrm{C}}(1 + (-1)^{h+k} + (-1)^{h+l} + (-1)^{k+l}) \\ & + f_{\mathrm{C}} e^{\frac{\pi}{2} i(h+k+l)} (1 + (-1)^{h+k} + (-1)^{h+l} + (-1)^{k+l}). \end{aligned}$$

This can be rewritten as:

$$F_{hkl} = 2 f_{\mathrm{C}} e^{\frac{\pi}{2} i(h+k+l)} \cos\left(\frac{\pi}{4}(h+k+l)\right) \times (1 + (-1)^{h+k} + (-1)^{h+l} + (-1)^{k+l}),$$

from which we find for the intensity:

$$I_{hkl} = 4 f_{\mathrm{C}}^2 \cos^2\left(\frac{\pi}{4}(h+k+l)\right) \times (1 + (-1)^{h+k} + (-1)^{h+l} + (-1)^{k+l})^2.$$

In addition to being zero for all reflections for which h,k,l are of different parity, this factor is also zero whenever $h+k+l = 4n+2$ with n an integer.

From these examples we conclude that absent reflections in a diffraction pattern give valuable information about the location of atoms in the unit cell, and about the presence of certain symmetry elements.

12.3 Intensity calculations for diffracted and measured intensities

When we perform an X-ray diffraction experiment, we typically measure the diffracted intensity for a certain period of time and with a detector with

a certain aperture. The measured intensity thus represents a time average (or an integration) of the scattered intensity and we only measure a small fraction of the total scattered intensity, because of the finite dimensions of the detector. In the following sections, we will describe a number of correction factors that must be included to compute the *measured* intensity, rather than the *diffracted* intensity. We will limit ourselves to the standard powder diffraction geometry described in the previous chapter, since that is the most commonly used phase identification method. Intensity computations for Scherrer patterns proceed along similar lines, whereas the intensities of reflections in Laue patterns require a more complicated approach (e.g., (Marín and Diéguez, 1999)).

12.3.1 Description of the correction factors

12.3.1.1 Temperature factor

Atoms in a crystal are not rigidly attached to their lattice sites. They move around their lattice sites in a (mostly) random fashion. The amplitude of this motion is determined by the available energy, which in turn is determined by the temperature. If the temperature of a solid increases, then the atoms will vibrate with a larger amplitude. At very low temperatures, the available energy is much smaller and therefore the atoms will be, on average, closer to their *equilibrium* positions.

If an atom vibrates with a certain amplitude, then its electron cloud will, on average, appear to be much larger and more diffuse than if the atom were stationary at one point. A larger electron cloud with the same number of electrons means that the electron density becomes slightly smaller, and this affects the value of the atomic scattering factor, f. This can be understood by considering the definition of f, as the ratio of the scattered amplitude of the total atom to that of one single electron. The theory of lattice vibrations is very complex and requires sophisticated mathematical techniques far beyond the level of this book. For our purposes, it will be sufficient to state the result: the atomic scattering factor must be multiplied by an exponential attenuation or damping factor, generally known as the *Debye–Waller factor*. Mathematically stated, we find:

$$f_T\left(\frac{\sin\theta}{\lambda}\right) = f_0\left(\frac{\sin\theta}{\lambda}\right) \mathrm{e}^{-B(T)\left(\frac{\sin\theta}{\lambda}\right)^2} = f_0(s)\mathrm{e}^{-B(T)s^2},$$

where the subscript 0 on the scattering factor indicates that the value at temperature $T = 0\,\mathrm{K}$ must be taken. The factor B is a function of temperature T and is proportional to the mean square displacement of the atom in a

Table 12.5. Debye–Waller factors $B(T)$ in Å^2 for a few elemental crystals (Peng *et al.*, 1996). These numbers must be multiplied by 0.01 to convert them to nm^2.

T (K)	Al *fcc*	Ti *hcp*	Fe *fcc*	Fe *bcc*	Cu *fcc*	Ag *fcc*	W *bcc*	Au *fcc*
90.0	0.3374	0.1579	0.1493	0.1715	0.1692	0.2259	0.0491	0.1908
130.0	0.3465	0.2281	0.1443	0.2476	0.2444	0.3262	0.0709	0.2755
170.0	0.4531	0.2982	0.1886	0.3238	0.3196	0.4265	0.0927	0.3602
210.0	0.5596	0.3684	0.2330	0.3999	0.3947	0.5267	0.1145	0.4448
260.0	0.6928	0.4560	0.2884	0.4950	0.4886	0.6517	0.1417	0.5503
270.0	0.7194	0.4735	0.2995	0.5140	0.5073	0.6767	0.1471	0.5714
280.0	0.7460	0.4911	0.3106	0.5330	0.5261	0.7017	0.1526	0.5925

direction normal to the reflecting plane.[2] The net effect of temperature is that every atom scatters less strongly than it would at absolute zero. The exponential attenuation factor is often written as e^{-M}, with $M = B(T)s^2$. The intensity of a diffracted beam is thus reduced by a factor e^{-2M} with respect to the intensity of that beam at absolute zero.

The theory behind the Debye–Waller factor is quite involved and requires knowledge of the *phonon density of states*, i.e., the number of lattice vibrations (or phonons) with a given frequency or wave length. Such computations are far beyond the level of this textbook, so, instead, we simply list $B(T)$ for a few pure elements with different crystal structures in Table 12.5. A more complete listing can be found in Peng *et al.* (1996).

On page 298, we computed the atomic scattering factor for tungsten, when Cu Kα radiation diffracts from the (222) planes of a *bcc* crystal with lattice parameter 3.1653Å; the result was $f_0 = 39.9358$. If we include the Debye–Waller correction factor, for $T = 290$ K (room temperature), then we find that

$$f = f_0 e^{-B(270)s^2} = 39.9358 \times 0.9538 = 38.0908.$$

The Debye–Waller factors are unknown for most crystal structures. If experimental values for the Debye–Waller factors are unavailable, then one could use the elemental values as rough estimates. From the data listed in Peng *et al.* (1996), it can be seen that, in general, the Debye–Waller factor is larger for elements in the left-most columns of the periodic table. At room temperature, values around 0.1 nm^2 would be quite reasonable for first column

[2] We are assuming that the atomic vibration amplitude is isotropic, i.e., it is the same in all directions. While this is a good approximation for close-packed (metallic) structures, in many other cases we must allow for the vibration amplitude to be different in different directions. The Debye–Waller factor is then described by a *vibration ellipsoid*, a 3-D shape that indicates in which direction(s) the maximal vibration amplitude occurs. For our purposes, we will always assume an isotropic atomic vibration pattern.

elements (Li, Na, K, Rb, Cs), whereas for second column elements (Be, Mg, Ca, Sr, Ba) values around 0.01–0.03 nm^2 are reasonable. For most other elements, values in the range 0.003–0.007 nm^2 are acceptable. At liquid nitrogen temperature, the Debye–Waller factors are typically about one-third of their room temperature values. The Debye–Waller factors for the elemental solids decrease down a column of the periodic table. If experimental values for $B(T)$ are available, then these should be used instead of the estimated values. Moreover, it is probably not a good idea to use an isotropic Debye–Waller factor in all situations.

12.3.1.2 Absorption factor

As X-rays travel through a sample, they are partially absorbed. Mathematically, this means that the total diffracted intensity must be multiplied by an *absorption factor* A. The value of A depends on the thickness of the material through which the beam has travelled and, in general, also on the shape of the sample. In addition, the absorption factor can depend on the diffraction angle θ, and one usually writes $A = A(\theta)$. Note that it is the *intensity*, not the amplitude, that must be multiplied by A.

One can show (see, for instance, (Cullity, 1978), page 134 for a detailed proof) that for the standard powder diffractometer, the absorption factor is independent of the diffraction angle and equal to:

$$A = \frac{1}{2\mu},$$

with μ the linear absorption coefficient of the specimen.

For a Debye–Scherrer camera, the absorption constant is more complicated to compute; for a cylindrical sample, however, one can show that the absorption is large for small diffraction angles and small for large angles. The thermal effect discussed in the previous section gives rise to an opposite behavior of the correction factors, so that the thermal correction and the absorption correction nearly cancel each other out. For other methods, in particular single crystal methods, absorption corrections can become rather involved since the absorption factor depends strongly on the sample shape, which is not always a simple shape, such as a sphere or a cylinder. For more details on absorption corrections, we refer the interested reader to (Cullity, 1978, Giacovazzo, 2002a).

12.3.1.3 Multiplicity factor

The modulus squared of the structure factor is proportional to the total diffracted intensity, scattered in a certain direction. However, for scattering from, say, the (200) plane in a Cu powder sample, there will also be scattering *in the same direction* from the (020) and (002) planes and their negatives. For planes with larger Miller indices, there are in general more possibilities. The total number of equivalent planes is known as the *multiplicity* of that

Table 12.6. Multiplicities for general and special planes in all crystal systems. The notation lists the Miller indices above and the multiplicity below the line: hkl/p_{hkl}.

Cubic	$\frac{hkl}{48}$	$\frac{hhl}{24}$	$\frac{0kl}{24}$	$\frac{0kk}{12}$	$\frac{hhh}{8}$	$\frac{00l}{6}$	
Hex./Rhom.	$\frac{hk.l}{24}$	$\frac{hh.l}{12}$	$\frac{0k.l}{12}$	$\frac{hk.0}{12}$	$\frac{hh.0}{6}$	$\frac{0k.0}{6}$	$\frac{00.l}{2}$
Tetragonal	$\frac{hkl}{16}$	$\frac{hhl}{8}$	$\frac{0kl}{8}$	$\frac{hk0}{8}$	$\frac{hh0}{4}$	$\frac{0k0}{4}$	$\frac{00l}{2}$
Orthorhombic	$\frac{hkl}{8}$	$\frac{0kl}{4}$	$\frac{h0l}{4}$	$\frac{hk0}{4}$	$\frac{h00}{2}$	$\frac{0k0}{2}$	$\frac{00l}{2}$
Monoclinic	$\frac{hkl}{4}$	$\frac{h0l}{2}$	$\frac{00l}{2}$				
Triclinic	$\frac{hkl}{2}$						

plane. Multiplicity is represented by the integer number p_{hkl}, and depends on the crystal symmetry. Table 12.6 lists the multiplicities for all planes in all crystal systems. As an example, consider the (220) planes in a cubic crystal. The table states that for reflections of the type $(0kk)$, the multiplicity is equal to 12; for the (224) planes we have $p_{224} = 24$. The total intensity scattered from a plane (hkl) must be multiplied by p_{hkl} to obtain the total intensity scattered in the direction corresponding to the angle $2\theta_{hkl}$.

12.3.1.4 Lorentz polarization factor

We have seen in the first section of this chapter that an unpolarized beam of X-rays is scattered differently in different directions, even by a single electron. The trigonometric factor describing this effect is given by:

$$P(\theta) = \frac{1 + \cos^2 2\theta}{2}.$$

There are three additional geometric factors that influence the total intensity in a diffracted beam. A powder crystal diffracts X-rays onto conical surfaces with tops in the center of the Ewald sphere and opening angles equal to the diffraction angles 2θ (see Fig. 11.19(b) on page 284). The total diffracted intensity scattered by the (hkl) planes is thus distributed over a conical surface. However, when we use a detector, either for powder diffractometry or in the form of the Debye–Scherrer camera, then we only intercept a fraction of this total diffracted intensity. For instance, for a Debye–Scherrer camera of radius R, the radius of the cone at the point where it intersects the photographic film is $R \sin 2\theta$. The total length of the diffraction line (circumference of the circle) is then $2\pi R \sin 2\theta$. The intensity per unit length of diffraction line is, therefore, proportional to $1/\sin 2\theta$; close to $2\theta = 0°$ or $180°$, the diffraction circles are small (see Fig. 11.19(c)) and the intensity per unit line length is high, whereas for angles close to $90°$ the intensity per unit line length becomes much smaller. This provides a first trigonometric correction factor of $1/\sin 2\theta$.

Consider next a powder sample with randomly oriented grains. The number of grains that are oriented close to a particular Bragg angle, θ, depends on the

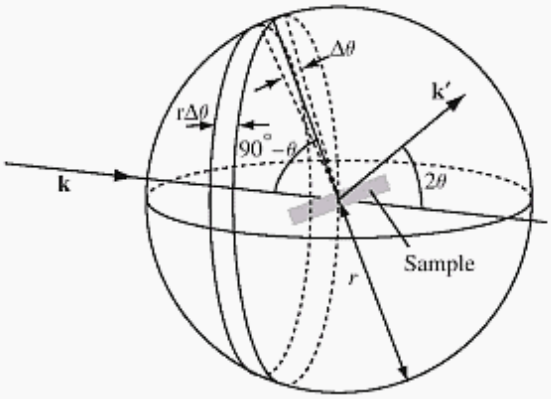

Fig. 12.6. Schematic illustration of the dependence of the number of grains close to a particular Bragg angle on that angle (see text for explanation; this figure is based on Fig. 4.16 in (Cullity and Stock, 2001)).

value of that angle. Let us assume that we are measuring the total intensity of a reflection with diffraction angle 2θ (see Fig. 12.6). The corresponding planes have plane normals that make an angle $90° - \theta$ with respect to the incoming beam. If the X-ray detector measures all the intensity over an angular interval $2\theta \pm \Delta\theta/2$, then the normal to the planes may vary from $90° - \theta - \Delta\theta/2$ to $90° - \theta + \Delta\theta/2$. If we consider the intersection of the plane normals with a sphere of radius r, centered in the origin of reciprocal space, then the plane normals of the planes giving rise to measurable diffracted intensity lie within a band of width $r\Delta\theta$ on the surface of this sphere. For randomly oriented grains, the end points of the plane normals will be uniformly distributed over the entire surface of this sphere. Therefore, the fraction of grains diffracting into the detector is equal to the ratio of the number of grains with normals inside the band, ΔN, to the total number of grains, N. This ratio, in turn, is equal to the ratio of the surface area of the band to the total area of the sphere:

$$\frac{\Delta N}{N} = \frac{r\Delta\theta . 2\pi r \sin(90° - \theta)}{4\pi r^2} = \frac{\Delta\theta \cos\theta}{2}.$$

The total number of grains oriented favorably for diffraction with an angle 2θ is thus proportional to $\cos\theta$, which is the second trigonometric correction factor.

The third correction factor is due to the fact that a set of planes does not diffract X-rays only at the exact Bragg orientation, but also when the orientation deviates slightly from the correct angle. This is easy to understand as follows: assume that a set of planes has Bragg angle θ. When the incident beam is in Bragg orientation, X-rays reflected from consecutive planes in the crystal are completely in-phase. If the incident beam is then tilted by a small angle $\Delta\theta$, the phase difference between consecutive planes in the crystal will change by a small amount as well. When $\Delta\theta$ is small, this phase difference will not be large enough to cause complete destructive interference, but the interference is not completely constructive either. Therefore, the intensity of the diffracted beam will be non-zero, but less than the intensity at exact Bragg orientation. The more planes that are present in the crystal, i.e., the larger the

grain size, the smaller the range of $\Delta\theta$ values for which some intensity can be observed. As we move the X-ray detector through the Bragg angle, we will begin to measure some intensity at $2(\theta - \theta')$; this intensity will reach a maximum value at 2θ, and then decrease again until it vanishes at $2(\theta + \theta'')$ (see Fig. 12.7). We define the *integrated intensity* as the total intensity over the entire angular range.

There are two commonly used mathematical functions that describe the peak shape: the *Gaussian function* and the *Lorentzian function*. They are defined as:

$$I^{\text{Gaussian}}(\alpha) = I_0 \exp\left[-4\ln 2\left(\frac{\alpha - 2\theta}{w}\right)^2\right]; \tag{12.13}$$

$$I^{\text{Lorentzian}}(\alpha) = \frac{I_0}{1 + 4\left(\frac{\alpha - 2\theta}{w}\right)^2}, \tag{12.14}$$

where I_0 is the maximum intensity, w is the full-width-at-half-maximum (FWHM), and α is the diffraction angle. The curves in Fig. 12.7 are shown for the following parameter values: $[2\theta = 40°, w = 2°, I_0 = 100]$ for the Gaussian function and $[2\theta = 50°, w = 1°, I_0 = 100]$ for the Lorentzian function. The Gaussian function drops off rapidly away from the maximum, whereas the Lorentzian peak has longer tails.

It can be shown (e.g., Cullity and Stock, 2001) that the FWHM value of a diffraction peak is related to the size of the grains that give rise to that peak and also to the value of the Bragg angle, θ. The relation is known as *Scherrer's formula* and reads as follows for grains with average diameter D:

$$w = \frac{0.9\lambda}{D\cos\theta}. \tag{12.15}$$

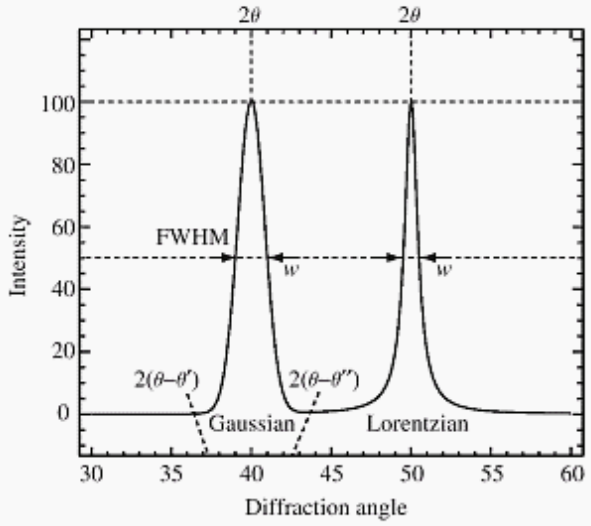

Fig. 12.7. Schematic illustration of the shape of a diffraction peak for two peak functions: Gaussian (left) and Lorentzian (right).

The smaller the grain size, the wider the diffraction peak. This relation can be used to determine approximate grain sizes for nano-crystalline materials.

If we approximate the integrated intensity by a rectangle, wI_0, we find from Eq. 12.15 that the width of the rectangle varies as $1/\cos\theta$. The height, I_0, of the rectangle also depends on θ, and it can be shown (Cullity and Stock, 2001, Fultz and Howe, 2002) that the dependence takes on the form $1/\sin\theta$. The integrated intensity of a diffraction peak is, therefore, proportional to the product of $1/\cos\theta$ and $1/\sin\theta$, so that the third correction factor is $1/\sin 2\theta$ (ignoring constant factors). Combining all three correction factors with the polarization factor we find that the intensity diffracted by an angle 2θ is proportional to:

$$\boxed{L_p(\theta) = \frac{1+\cos^2 2\theta}{\sin^2\theta\cos\theta}.} \tag{12.16}$$

This expression is known as the *Lorentz polarization factor*, and it is shown graphically in Fig. 12.8. Note that this factor is significantly different from 1, and must be taken into account in any intensity computation.

12.3.2 Expressions for the total measured intensity

The total intensity can now be computed by putting together all contributing factors and correction factors. It is standard practice in most diffraction experiments to measure all intensities, and then re-scale them so that the most intense peak has intensity 100. In doing so, one effectively cancels the incident intensity I_0, the constant K, the distance r from the observer to the sample, and a number of other factors that are common to all reflections. The relevant part of the intensity of a diffracted beam is, therefore, given by:

$$\boxed{I_{hkl} = |F_{hkl}|^2 p_{hkl} L_p(\theta) A(\theta) e^{-2M}.} \tag{12.17}$$

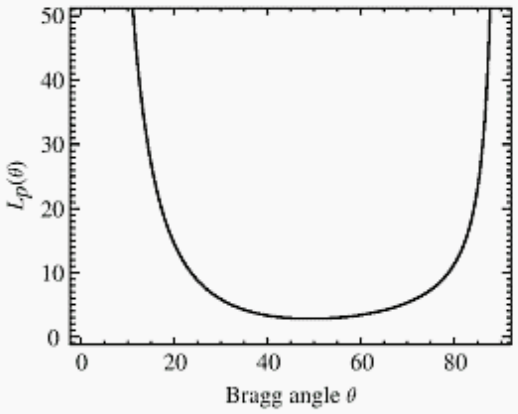

Fig. 12.8. Lorentz polarization factor $L_p(\theta)$.

Table 12.7. Computation of integrated intensities for polycrystalline tungsten.

Line	(hkl)	d_{hkl} (Å)	$\sin\theta$	θ (rad)	s (Å^{-1})	$f_{hkl}(s)$	e^{-M}	$L_p(\theta)$	p
1	110	2.2381	0.3445	0.3517	0.2234	59.5101	0.9921	14.1997	12
2	200	1.5826	0.4871	0.5088	0.3159	52.9576	0.9843	6.1572	6
3	211	1.2921	0.5966	0.6393	0.3870	48.2587	0.9766	3.7912	24
4	220	1.1190	0.6889	0.7600	0.4468	44.6851	0.9689	2.9144	12
5	310	1.0009	0.7702	0.8792	0.4996	41.9907	0.9613	2.7349	24
6	222	0.9137	0.8437	1.0042	0.5472	39.9344	0.9538	3.0871	8
7	321	0.8459	0.9114	1.1466	0.5911	38.3054	0.9463	4.2034	48
8	400	0.7913	0.9743	1.3435	0.6319	36.9457	0.9388	8.4479	6

Table 12.8. Computation of integrated intensities for polycrystalline tungsten (continued).

Line	$\lvert F_{hkl}\rvert^2 e^{-2M}$	Intensity	2θ (°)	Relative intensity	Experiment (PDF# 040806)
1	13943.997	2376009	40.30	100.0	100
2	10869.570	401555	58.31	16.9	21
3	8884.827	808416	73.26	34.0	40
4	7498.409	262237	87.09	11.0	16
5	6517.732	427815	100.75	18.0	25
6	5802.711	143309	115.08	6.0	10
7	5255.362	1060339	131.39	44.6	48
8	4812.331	243924	153.95	10.3	6

For a powder diffractometer one can remove the absorption factor $A(\theta)$ from the expression since it is constant and will cancel out when the integrated intensities are re-scaled to the most intense reflection.

Let us consider an explicit example: tungsten, body-centered cubic with lattice parameter $a = 0.31653$ nm, for Cu-Kα radiation at $T = 290$ K; the Debye–Waller factor B is equal to 0.1581 Å^2 (Peng *et al.*, 1996). To compute the diffracted intensities for a powder diffraction pattern, it is convenient to work in table format, as shown in Tables 12.7 and 12.8. The computation is relatively easy if one works through the tables one column at a time. Spreadsheet programs are useful for these types of calculations.

The last column in Table 12.8 is taken from the Powder Diffraction File, card # 040806, which lists the experimental relative intensities for the eight reflections observed in the 2θ range $[0° - 180°]$.[3] The agreement between

[3] Since the calculated values assume that the illuminated area on the sample remains constant for the entire angular range, the values from the Powder Diffraction File were corrected so that they represent a variable slit diffractometer (i.e., we used *Int-v* values).

the relative intensities is reasonably good, considering that the experimental values represent peak intensities, not integrated intensities. In Chapter 14, we will consider a more explicit example where we compare the calculated integrated intensities with experimental integrated intensities for an NaCl powder sample.

The computation of diffracted intensities for the Laue geometry is more complicated than for the powder pattern, due to the continuous wave length range. For a detailed description of Laue intensity computations, we refer the interested reader to Marín and Diéguez (1999).

12.4 Historical notes

Wilhelm Konrad Röntgen (1845–1923) was a German scientist who, in 1895, discovered X-rays. He was born in Lennep in the German Rhineland and was the son of a cloth merchant and manufacturer. He moved to Holland at an early age and in 1862 attended the Ultrecht Technical School and later the Polytechnical School in Zürich. He was a professor of physics at the University of Würzburg and director of its physical institute when, in 1895, he discovered X-rays using a Crookes vacuum cathode tube (Röntgen, 1896). Röntgen also pursued the study of the electrical conductivity and heat expansion of crystals. It was his discovery of X-rays, however, that paved the way for future scientists to study the atomic structure in the crystalline solid state.

Max Theodor Felix von Laue (1879–1960) was a German physicist and crystallographer who made many contributions to the theory and practice of X-ray diffraction. He was a professor at the University of Munich. He was the first to observe X-ray diffraction (1912) from copper sulfate. This discovery

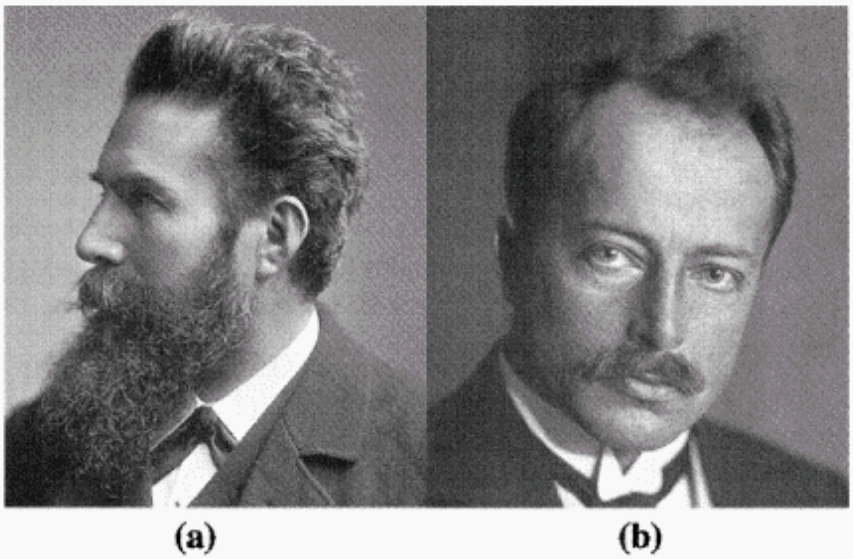

Fig. 12.9. (a) William Konrad Röntgen (1845–1923), and (b) Max Theodor Felix von Laue (1879–1960) (pictures courtesy of the Nobel Museum).

opened the door to many future studies of the structure of the solid state. Laue's discussions with Ewald on scattering of X-rays from 3-D gratings with a periodicity close to that of the X-ray wave length, stimulated his experiments to demonstrate the diffraction of X-rays by crystals. He developed what is now known as the Laue method for X-ray diffraction.

12.5 Problems

(i) *Symmetry related extinctions*: Derive the extinctions that are implied for the following symmetry operations:

(a) A 2_1 screw axis parallel to the a-direction.
(b) Absences in $(hk0)$ reflections for a b-glide parallel to the (001) plane.

(ii) *Structure factor I*: Consider an *hcp* cell with identical atoms in the $2c$ position of space group $\mathbf{P6_3/mmc}$ (D^4_{6h}) at $(1/3, 2/3, 1/4)$ and $(2/3, 1/3, 3/4)$.

(a) Show that the atomic positions can be expressed equivalently as: (0,0,0) and $(1/3, 2/3, 1/2)$.
(b) Show that the structure factor can be expressed as:

$$F_{hkl} = f_{atom}\left(1 + e^{2\pi i\left[\frac{h+2k}{3} + \frac{l}{2}\right]}\right).$$

(c) Calculate the square modulus of this structure factor $F^2_{hkl} = F_{hkl}F^*_{hkl}$.
(d) Express the square modulus of the structure factor for each of the following four cases:

- $h + 2k = 3n$, $l =$ even;
- $h + 2k = 3n \pm 1$, $l =$ odd;
- $h + 2k = 3n \pm 1$, $l =$ even;
- $h + 2k = 3n$, $l =$ odd.

(e) Co has two polymorphic forms, *hcp* and *fcc*. Describe extinction conditions that could be used to distinguish the reflections from the *hcp* and *fcc* phases, respectively.

(iii) *Structure factor II*: GaAs adopts a *fcc* structure with Ga atoms at the $(0, 0, 0)$ and As at the $(1/4, 1/4, 1/4)$ special positions.

(a) Express the positions of all atoms in the unit cell.
(b) Express the structure factor for GaAs.
(c) Express the square modulus of the structure factor.

(d) Simplify the square modulus under the following conditions:

1. $h+k+l=2n+1$
2. $h+k+l=2(2n+1)$
3. $h+k+l=2n$.

(iv) *Structure factor III*: Consider the face-centered cubic BiF_3 structure, with Bi atoms on the $(0,0,0)$ special position, and F on $(1/2,1/2,1/2)$ and $(1/4,1/4,1/4)$ special positions of the space group $\mathbf{Fm\bar{3}m}$ (O_h^5). Derive a simple expression for the structure factor; are there any systematic absences other than those caused by the face centering?

(v) *Structure factor IV*: Consider the face-centered cubic CaF_2 structure, with Ca atoms on the $(0,0,0)$ special position, and F on $(1/4,1/4,1/4)$ special positions of the space group $\mathbf{Fm\bar{3}m}$ (O_h^5). Derive a simple expression for the structure factor; are there any systematic absences other than those caused by the face centering? How does this structure factor differ from that of the BiF_3 structure in the previous problem?

(vi) *Integrated intensities I*: Repeat the computation of the integrated intensities of Tables 12.7 and 12.8 for the structures described in the preceding two problems. You may ignore the Debye–Waller factors (i.e., put $e^{-M}=1$).

(vii) *Integrated intensities II*: Consider the NaCl structure, with lattice parameter 0.5639 nm, space group $\mathbf{Fm\bar{3}m}$ (O_h^5), Na at $(0,0,0)$ and Cl at $(1/2,1/2,1/2)$. Compute the ratio of the integrated intensities for the 111 and 200 reflections as a function of the position of the Cl atom, when this atom is translated linearly from the position $(1/2,1/2,1/2)$ to the position $(1/4,1/4,1/4)$. Hint: define a parameter q so that $q=1$ corresponds to $(1/2,1/2,1/2)$ and $q=0$ to $(1/4,1/4,1/4)$; then express the structure factor as a function of q and compute the integrated intensities.